Evolution from the vortex state to the critical state in a square-columnar Josephson-junction array

D.-X. Chen, J. J. Moreno, and A. Hernando
Instituto de Magnetismo Aplicado, RENFE-UCM, 28230 Las Rozas, Madrid, Spain

(Received 15 May 1995)

The remanence of a 25×25 square-columnar Josephson-junction array with normalized maximum junction current $i_{\max}$ is calculated from the dc and ac Josephson equations, the Ampère theorem, and the gauge invariance. It is shown that with increasing $i_{\max}$ the remanence changes from zero to nonzero. The field profile in the nonzero remanence state has multiple peaks at smaller $i_{\max}$ but a single peak at greater $i_{\max}$, indicating a transition from the vortex state to the critical state.

I. INTRODUCTION

It is recognized that there is a Josephson vortex (JV) structure in long Josephson junctions (JJ's) and large JJ arrays. Similar to the Abrikosov vortex (AV) in type-II superconductors,[1] an ideal JV presents a field peak containing a flux quantum Φ_0 which is produced by a current vortex.[2] Therefore, in the literature, when a critical state is found in a JJ system (e.g., in the intergranular matrix of high-T_c superconductors[3–6]), its origin is frequently attributed to JV pinning by defects, just like the AV pinning in type-II superconductors.

On the other hand, there is an advantage in the study of JJ systems; their electromagnetic properties as a whole can be thoroughly calculated directly from fundamental principles, unlike the case of type-II superconductors, where several phenomenological theories have to be used for different partial properties, such as thermal equilibrium magnetization,[1,7,8] surface barriers,[9] and critical currents.[10] Compared with using an analogy between JJ systems and type-II superconductors, it should be more reliable to study the critical state in JJ systems by direct calculations. In this work, we calculate the field profile of a uniform 25×25 square-columnar JJ array in its remanence state. We will show how a vortex state can be changed to a critical state just by increasing the JJ critical current and describe the features of both states.

II. MODEL AND CALCULATION

The studied JJ array has the same geometry as that treated in Ref. 11. The xy-plane cross section of an array of superconducting grains, whose z dimensions are infinitely long, forms a 25×25 square lattice of parameter a_0, each grain being centered at (i,j), with $i=1,2,\ldots,25$ and $j=1,2,\ldots,25$. Every two nearest grains are weak-linked by a JJ, which has a constant maximum dc Josephson current $I_{\max}$ and normal resistance R per meter length.[12] Four nearest grains with a centered void form a square cell; the effective void area being A_V. We name the gauge-invariant phase differences for JJ's along the x and y axes θ_{ij} and ϑ_{ij}, respectively. The index of the phase difference ij for a JJ is defined the same as one of the two grains weak-linked by it that has a smaller i or j. The positive currents (and the positive phase differences) are defined in the x and y directions. Thus, when external field H is applied in the z direction, the following differential equation system for the 1200 gauge-invariant phase differences of all JJ's is built up based on the dc and ac Josephson equations, and the Ampère theorem:

$$\frac{d\theta_{ij}}{dt^*}=-2\pi h+\theta_{ij}-\theta_{i,j+1}-\vartheta_{ij}+\vartheta_{i+1,j}-2\pi i_{\max}\sin\theta_{ij}\quad(1\leqslant i\leqslant 24,\ j=1),$$

$$\frac{d\theta_{ij}}{dt^*}=-\theta_{i,j-1}+2\theta_{ij}-\theta_{i,j+1}-\vartheta_{ij}+\vartheta_{i,j-1}-\vartheta_{i+1,j-1}+\vartheta_{i+1,j}-2\pi i_{\max}\sin\theta_{ij}\quad(1\leqslant i\leqslant 24,\ 2\leqslant j\leqslant 24),$$

$$\frac{d\theta_{ij}}{dt^*}=2\pi h-\theta_{i,j-1}+\theta_{ij}+\vartheta_{i,j-1}-\vartheta_{i+1,j-1}-2\pi i_{\max}\sin\theta_{ij}\quad(1\leqslant i\leqslant 24,\ j=25),$$

$$\frac{d\vartheta_{ij}}{dt^*}=2\pi h+\vartheta_{ij}-\vartheta_{i+1,j}-\theta_{ij}+\theta_{i,j+1}-2\pi i_{\max}\sin\vartheta_{ij}\quad(i=1,\ 1\leqslant j\leqslant 24),$$

$$\frac{d\vartheta_{ij}}{dt^*}=-\vartheta_{i-1,j}+2\vartheta_{ij}-\vartheta_{i+1,j}-\theta_{ij}+\theta_{i-1,j}-\theta_{i-1,j+1}+\theta_{i,j+1}-2\pi i_{\max}\sin\vartheta_{ij}\quad(2\leqslant i\leqslant 24,\ 1\leqslant j\leqslant 24),$$

$$\frac{d\vartheta_{ij}}{dt^*}=-2\pi h-\vartheta_{i-1,j}+\vartheta_{ij}+\theta_{i-1,j}-\theta_{i-1,j+1}-2\pi i_{\max}\sin\vartheta_{ij}\quad(i=25,\ 1\leqslant j\leqslant 24).\tag{1}$$

In these equations, t^* is the normalized time t to the nominal time constant τ of one cell and h and $i_{\max}$ are the normalized H and $I_{\max}$ to $\Phi_0/\mu_0 A_V$:

$$t^*=t/\tau=tR/L=tR/\mu_0 A_V,\tag{2}$$

0163-1829/96/53(10)/6579(6)/$10.00

$$h = \mu_0 A_V H / \Phi_0, \tag{3}$$

$$i_{max} = \mu_0 A_V I_{max} / \Phi_0, \tag{4}$$

where L is the self-inductance of a cell per meter length and Φ_0 the flux quantum.[12]

Our aim is to calculate the field in all voids, $\{H_{ij}\}$, normalized to $\Phi_0 / \mu_0 A_V$ when $h = 0$:

$$h_{ij} = (\theta_{ij} + \vartheta_{i+1,j} - \theta_{i,j+1} - \vartheta_{ij})/2\pi \quad (i,j = 1,2,\ldots,24). \tag{5}$$

Its index ij is that of the grain in the same cell with smaller i and j.

To obtain a solution for the remanence state, we start from $\{\theta_{ij} = \vartheta_{ij} = 0\}$ ($\{h_{ij} = 0\}$), increase stepwise h from 0 to a maximum value h_{max} and calculate the fully relaxed $\{h_{ij}\}$, and then decrease stepwise h back to 0 and calculate again the fully relaxed $\{h_{ij}\}$, which is our final solution.

The numerical calculations were performed using a Runge-Kutta method with small t^* steps between 0.1 and 0.002. To ensure each result to be the fully relaxed one, the absolute values of all the residual time derivatives of the phase differences in Eqs. (1) were less than αi_{max} with $\alpha = 10^{-8}$ to 10^{-10}. Also, as a routine check, we compared the resulted $\{h_{ij}\}$ with itself after a 90° and 180° rotation around the central infinite axis and after a mirror-image operation respect to its midplane and diagonal plane containing

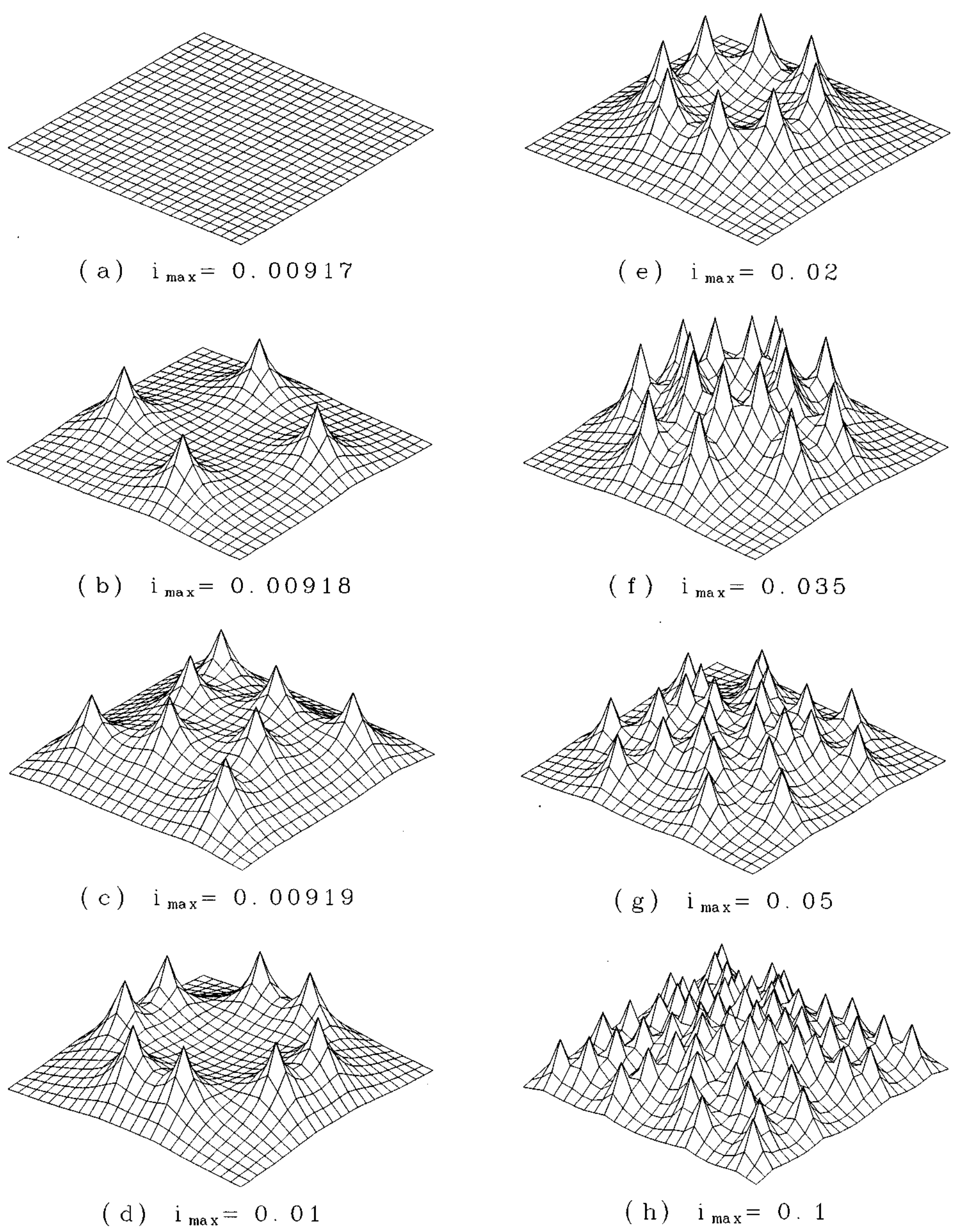

FIG. 1. The intergranular field profiles of the 25×25 square-columnar Josephson-junction array at saturated remanence for different values of i_{max}. In order to show clearly the profiles and to have a quantitative comparison among them, the scale factors of field are chosen as 250 for (a)–(c), 0.5 for (n)–(p), and 150, 100, 50, 25, 15, 5, 2.5, 1.5, and 1 for (d)–(m), successively. It can be observed that JV's have almost the same height when their density is low [(b)–(d)]; their height increases with increasing density [(e)–(h)]; and after a central maximum appears, the maximum field increases with increasing i_{max} [(i)–(p)]. However, this maximum remains the same when $1 \leqslant i_{max} \leqslant 1.6$ [(n) and (o)].

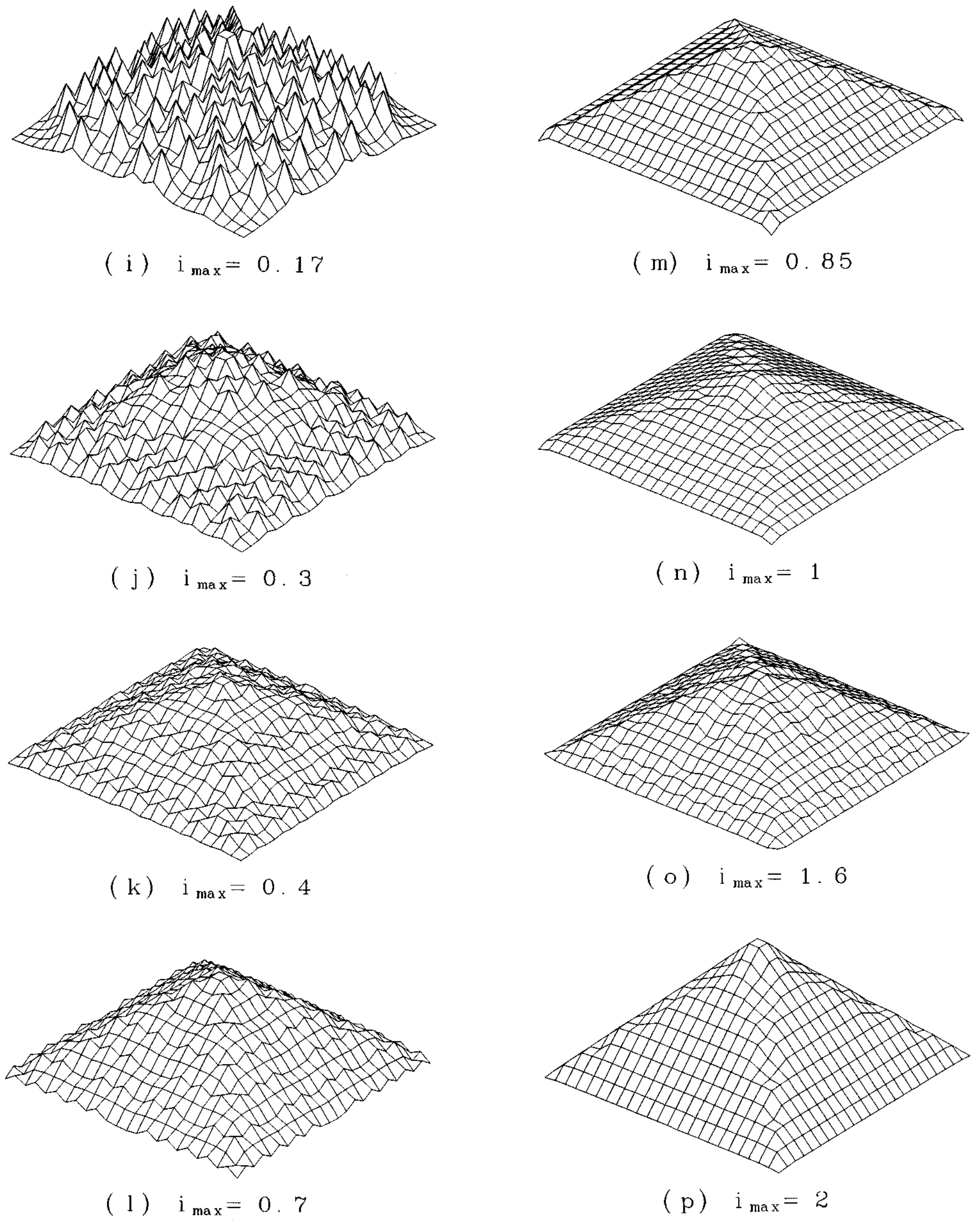

FIG. 1. (*Continued*).

the axis; the profile has a corresponding symmetry if their difference is very small.

III. RESULTS

The evolution of the calculated h_{ij} profile in the remanence state is shown in Figs. 1(a)–1(p) with $i_{\max}$ ranging from less than 0.009 17 to 2. In order to obtain a saturated remanence state, $h_{\max}$ was set to be 100, except for $i_{\max}=0.17$ and 0.3, where $h_{\max}=1$ and 10 were used, respectively. If $h_{\max}=100$, one-step procedures were performed when h changed from 0 to $h_{\max}$ and from $h_{\max}$ to 0; but if $h_{\max}=1$ and 10, many steps as small as 0.01 were used during increasing h, although its decrease was also taken to be one step.

When $i_{\max}\leqslant 0.009\,17$, the solution is always trivial with $h_{ij}=0$ for every i and j [Fig. 1(a)]. The field profile consists of peaks with practically the same height for $0.009\,18\leqslant i_{\max}\leqslant 0.1$ [Figs. 1(b)–1(h)]. The profiles for $i_{\max}\geqslant 0.17$ [Figs. 1(i)–1(p)] have a maximum field at the center, and have an overall pyramid shape if $i_{\max}\geqslant 0.4$ [Figs. 1(k)–1(p)].

As studied in Ref. 11, the symmetry of the field profiles of square-columnar JJ arrays is often not complete. Among the profiles shown in Figs. 1, ten [Figs. 1(a), (d–f), and (h–p)] have all four types of symmetry mentioned above. Among the remaining six, five [Figs. 1(b), (c), and (g–i)] have 90° and 180° rotation symmetries only, and the case of $i_{\max}=0.3$ has a unique 180° rotation symmetry. Since the geometric symmetry of the model configuration requires all the profiles to have as high degree of symmetry as possible, we have spent very long computer time to find it. Also, $h_{\max}$ for $i_{\max}=0.17$ and 0.3 has to be reduced quite a bit from 100 for saving time and the number of field steps had to be increased. We believe that all the plotted results correspond to those having the highest degree of symmetry possible.

IV. VORTEX STATE

A. Vortex state

The magnetic properties of uniform JJ's have been calculated from the sine-Gordon equation in Ref. 13. The results can be entirely interpreted in terms of JV's if both complete and incomplete JV's are considered. In other words, such JJ's are always in a vortex state. Different from the ideal soliton JV defined in an infinite JJ and zero applied field H as a field peak containing a flux quantum Φ_0 produced by its current vortex, the Φ_0 of a complete JV in finite uniform JJ's is produced not only by its current vortex but also by H and the current vortices of the incomplete JV's on the JJ edges. If there are several JV's present in one state, their field peaks are always identical with the same height and width.

The studied uniform JJ arrays of $i_{max} \leqslant 0.1$ have similar features to uniform JJ's, so that they are also in a vortex state.

B. Comparison with uniform junction and slablike array

The studied square-columnar JJ array is structurally different from the uniform JJ treated in Ref. 13 at least in two points: (i) The former is a discrete system with superconducting JJ's and normal voids, but the latter is a continuous JJ system. (ii) The former is mathematically two dimensional (2D), but the latter is one dimensional (1D). We have studied a finitely thick, infinitely wide and long slablike JJ array.[14] That array is a discrete system like the present square-columnar array, but its periodical structure with an infinite width makes it a mathematically 1D system like the uniform JJ. It will be interesting to compare the three systems in their JV state.

In the simplest finite 1D system, the uniform JJ, the dc Josephson equation with gauge-invariant phase difference leads to the simplest JV structure, as described in Sec. IV A. This 1D system is the continuous counterpart of one column of the slablike JJ array. Therefore, the JV structure in the 1D array should be compared with that in the uniform JJ only for one column; in the entire array, every current vortex corresponds to an infinite number of Φ_0, which results from the unrealistic infinite array width.[14] Changing 1D into 2D and keeping the same discreteness, the JV in the square-columnar array returns to the situation of uniform JJ's, having one Φ_0 each, since its flux quatization occurs along two perpendicular dimensions.

If we ignore the multi-Φ_0 character of JV in the 1D array, and consider one column only, we will find that the JV states in both 1D and 2D JJ arrays have the following common feature. Defined by a field peak containing one Φ_0, the border of a JV will be almost always across a number of voids, around which the JJ currents are shared by two adjacent JV's. Therefore, unlike in uniform JJ, the JV's in the array have a collective meaning, that is, a group of JV's contains a number of Φ_0's produced by a number of current vortices.[14]

Limited by the small i_{max} values, another significant difference between the arrays of large N and uniform JJ's was not shown in Ref. 13. It is the appearance of nonzero remanence in discrete systems, which has been studied in Ref. 11 for the square-columnar array. Most profiles present in Fig. 1 are for the nonzero remanence case with $i_{max} \geqslant 0.009\,18$. In this sense, we can say that the discreteness extends the field range to include $H=0$ for JV's to exist, and if $i_{max} \leqslant 0.009\,17$, the JV state in the array is more similar to the same state in uniform JJ's.

C. Complete and incomplete vortices

Inspecting the results in Fig. 1, we will find another feature of the square-columnar array, which is distinct from the other two JJ systems. Let us study the details of the JV state at remanence.

The remanence becomes nonzero at $i_{max}=0.009\,18$ with a four-peak profile [Fig. 1(b)]. After a slight increase in i_{max}, these peaks become closer to the center and surrounded by another group of four peaks, resulting in an eight-peak configuration [Fig. 1(c)]. Further increasing i_{max} reorganizes the eight peaks into a circular arrangement and the radius of the circle shrinks [Figs. 1(d) and 1(e)]. When i_{max} is increased to 0.035 and 0.05, a second and third circles of 8 peaks appear, so that the total peak number becomes 16 and 24, respectively [Figs. 1(f) and 1(g)]. At even greater i_{max} $(=0.1)$, the circular configuration changes into a roughly uniform one with 64 peaks [Fig. 1(h)].

Each field peak can contain a complete or fractional Φ_0, corresponding to a complete or incomplete JV, respectively. Different from the 1D array, where all the inner JV's are complete and all the outer JV's are incomplete at remanence, we can only say for the 2D array that some inner JV's in Fig. 1 are complete and all JV's the nearest and sometimes the second nearest to the sides are incomplete. Without a sudden change in configuration, the fraction increases with increasing i_{max}.

We give some calculated data to explain this. The fraction is 0.632 for the four-peak configuration when $i_{max}=0.00918$ [Fig. 1(b)], but it is only increased to an averaged fraction 0.657 for the eight-peak configuration when $i_{max}=0.009\,19$ [Fig. 1(c)]. Thus, the inner four JV's for the latter cannot be complete, since otherwise the outer four will have a fraction of less than 0.32, which contradicts the appearance of the outer peaks. Therefore, all inner and outer JV's are incomplete in Fig. 1(c). On the other hand, we see clearly the shrink of an eight-peak configuration in Figs. 1(d)–1(f) with increasing i_{max} from 0.01 to 0.35. The corresponding average fraction increases from 0.644 at $i_{max}=0.01$ to 0.883 at $i_{max}=0.02$ to 1 at $i_{max}=0.035$ for the inner JV's. We judge the last ones to be complete since the average fraction for all 16 peaks is as large as 0.930, and the side of each inner JV has no way to be extended to the array border without passing the outer peak. The situation is similar for the 24-peak configuration; the average fraction is 0.945 and all the inner JV's are complete. When $i_{max}=0.1$ in Fig. 1(h), the relative positions of the peaks are somewhat similar to Fig. 1(c), so that among the 64 JV's with an average fraction 0.791, the ones the nearest and second nearest to the boundary are incomplete and the others are complete.

V. CRITICAL STATE

A. Bean-like critical state

The field profiles shown in Figs. 1(i)–1(p) for $i_{max} \geqslant 0.17$ are obviously different from those with smaller

i_{max}. Instead of a number of peaks of the same height as in Figs. 1(b)–1(h), the field at the center has a maximum height. Especially, if $i_{max} \geqslant 0.4$, there is one peak only, which is pyramidlike with or without superimposed oscillations on the four sides.

The pyramid field peak is consistent with the critical-state model proposed by Bean.[15] This model assumes that the volume supercurrent flows in a hard superconductor with density J equal to the critical-current density J_c. A region or the entire superconductor are in the critical state if $|J| = J_c$ holds therein. For simplicity, Bean used a constant J_c to calculate magnetization. In this case, the field profile of a square column at its saturated remanence must be a pyramid with four planar sides of constant slope since the gradient of field equals the constant J_c owing to the Ampere theorem. Because the field profiles of the arrays with larger i_{max} have similar field profiles to that predicted by Bean's critical-state model, we call the state in the arrays of $i_{max} \geqslant 0.4$ the Bean-like critical state.

The critical-state model considers the current to flow continuously in a critical state, whereas the currents in the array can only flow through the discrete JJ's, the actual field profile in the array should be stepwise, which is not shown in the figures for simplicity. A big difference between the Bean critical state and the Bean-like critical state is displayed by the superimposed field oscillations for the latter when i_{max} is not integral [see the oscillations along the slope and parallel to the border in Fig. 1(k) and parallel to the board in Fig. 1(o)]. Even if the sides are smooth when i_{max} is integral, the slopes of the sides are never constant everywhere [see Figs. 1(n) and 1(p) for $i_{max} = 1$ and 2, where the slope close to the four edges is obviously different from that on the major part of the sides].

B. Stochastic transition

The significant difference in the field profiles between the arrays with $i_{max} \leqslant 0.1$ and $i_{max} \geqslant 0.4$ implies that a transition occurs when $0.1 < i_{max} < 0.4$. Actually, there is a stochastic transition in a 1D array of $N \to \infty$, occurring at $i_{max} = i^*_{max} = 0.9716 \ldots /2\pi \approx 0.155$.[16,17] In such a 1D array, there is not a general exact current and field periodicity like in uniform JJ's, and changes in profile shape can usually be found if a large number of cells is inspected. If i_{max} is very small, the current and field profiles are quite accurately periodic within a finite section of a sufficiently large number of cells. The period corresponds to a Φ_0, very similar to those in a continuous uniform JJ, so that JV's can be well defined. With increasing i_{max}, departures from such a periodicity will occur from section to section due to disconnected stochasticity, but the average current is always zero in the entire array, i.e., the current oscillates between positive and negative over large intervals. When i_{max} is increased to i^*_{max}, connected stochasticity starts to occur and a nonzero average current becomes possible in the entire array. Further increasing i_{max} will create possibilities to have a new type of periodical current with a nonzero average value i_c, the average critical current. Since the nonzero-i_c state is immerged among many different possible states in a connected stochastic sea, the transition occurring at $i_{max} = i^*_{max}$ is referred to as a stochastic transition.

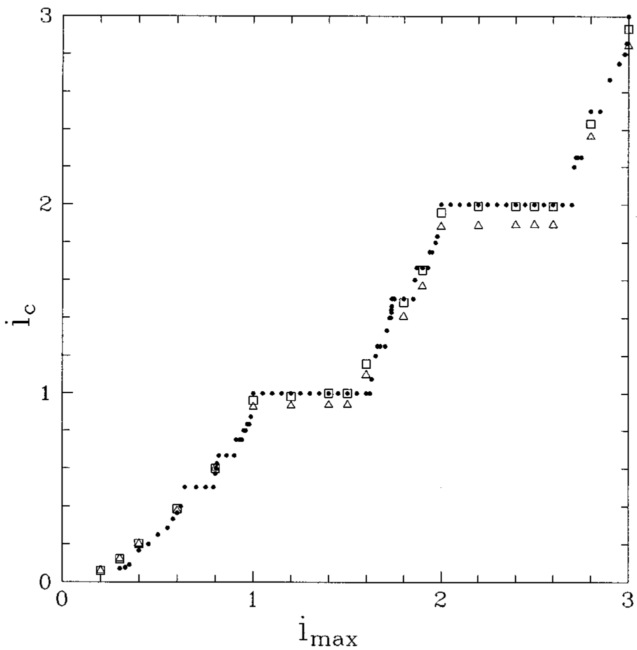

FIG. 2. The averaged critical current i_c as a function of i_{max}. ●, calculated for infinite 1D array (Refs. 16–19). △, calculated from h_{max} of 25×25 2D array using Eq. (6). □, calculated from ϕ of a 25×25 2D array using Eq. (7).

Our results show that although the studied array is a 2D array with finite N, a similar stochastic transition also occurs when $0.1 < i_{max} < 0.4$. Since there can be a nonzero i_c, which corresponds to J_c in the critical-state model, the pyramid field profiles are expected.

C. Critical-current density

We now compare quantitatively the critical state in our discrete JJ system with the continuous Bean critical state in terms of the correlation between i_c and J_c. In the array, the normalized J_c is $j_c = i_c/a_0$. From Bean's critical-state calculation, the normalized maximum field at the center of the square-columnar array is

$$h_{max} = j_c N a_0/2 = i_c N/2, \tag{6}$$

and the total flux normalized to Φ_0 is

$$\phi = \Phi/\Phi_0 = i_c N^3/6. \tag{7}$$

Using these two equations, we calculate the average i_c for the array from h_{max} and ϕ obtained from Eqs. (1). The results for $0.2 \leqslant i_{max} \leqslant 3$ are given in Fig. 2, where the i_c defined as the average JJ current within one period in the infinite 1D array is also plotted for comparison.[16–19] We can see an overall agreement among the three cases. Detailed comparison reveals that in most cases i_c of the finite 2D array obtained from ϕ agrees well with i_c of infinite 1D array, but when $i_{max} \leqslant 0.4$ the former is appreciably greater. i_c of the finite 2D array obtained from h_{max} is a few percent smaller than that obtained from ϕ when $i_{max} \geqslant 1$, but they are almost equal otherwise.

The perfect pyramid field profile of Bean's critical state at remanence is a consequence of static shielding owing to the Lenz law with a constant J_c. The imperfect pyramid field profile of the Bean-like critical state in the JJ array is a consequence of static shielding owing to the ac Josephson effect with a roughly constant average J_c.[20] Both the total flux ϕ and the maximum field $h_{\max}$ are produced by all JJ currents, so that i_c's calculated from them are the average JJ current over the JJ array. However, it is better to use i_c calculated from ϕ as the average current of the entire array, since the local field $h_{\max}$ is more influenced by the stepwise profile shape. The equal field in the four central voids as seen from Figs. 1(n)–1(p) makes i_c calculated from $h_{\max}$ lower. Thus, we conclude that when $i_{\max} \geqslant 0.6$, the average JJ current in the 2D array agrees well with i_c of the infinite 1D array. When $i_{\max} \leqslant 0.4$, the average current is much greater than i_c of the infinite 1D array. This is because the period of JJ current spans many cells so that the ac Josephson effect can choose JJ's with larger currents to be close to the array surface to realize the most effective static shielding. In this case, obvious circumferential plateaus are present on the sides of profile, resulting from the current oscillations of large amplitudes. We should mention that if the array size is greater, the agreement in i_c for the three cases will be better for $i_{\max} \geqslant 0.6$.

VI. CONCLUSION

The field profile of a 25×25 square-columnar Josephson-junction array has been calculated at saturated remanence. The profile varies with the nomalized junction critical current $i_{\max}$ defined by Eq. (4). If $i_{\max} \leqslant 0.1$, it contains peaks of equal height, presenting a vortex state. If $i_{\max} \geqslant 0.4$, it consists of a single pyramid peak, indicating a critical state. The transition from vortex to critical state in the two-dimensional array coincides with the stochastic transition in an infinite one-dimensional Josephson-junction array, and the averaged critical current of the latter can be used for accurate calculations of the critical-current density of the former if $i_{\max} \geqslant 0.6$.

ACKNOWLEDGMENTS

This work was partially supported by Spanish CICYT through Project Nos. MAT92-0405 and MAT92-0491.

[1] A. A. Abrikosov, Zh. Éksp. Teor. Fiz. **32**, 1442 (1957) [Sov. Phys. JETP **5**, 1174 (1957)].

[2] B. D. Josephson, Rev. Mod. Phys. **36**, 216 (1964).

[3] J. R. Clem, Physica C **153-155**, 50 (1988).

[4] M. Tinkham and C. J. Lobb, in *Solid State Physics*, edited by H. Ehrenreich and D. Turnbull (Academic, New York, 1989), Vol. 42, p. 91.

[5] K. H. Müller, Physica C **159**, 717 (1989).

[6] H. Dersch and G. Blatter, Phys. Rev. B **38**, 11 391 (1988).

[7] Z. Hao and J. R. Clem, Phys. Rev. B **43**, 7622 (1991).

[8] Z. Hao and J. R. Clem, Phys. Rev. Lett. **67**, 2371 (1991).

[9] C. P. Bean and J. D. Livingston, Phys. Rev. Lett. **12**, 14 (1964).

[10] P. W. Anderson and Y. B. Kim, Rev. Mod. Phys. **36**, 31 (1964).

[11] J. J. Moreno, D.-X. Chen, and A. Hernando, Phys. Rev. B **51**, 16 440 (1995).

[12] The maximum dc Josephson current $I_{\max}$ of a JJ is its critical current, I_c, at zero applied field. In our case there are nonzero fields at JJ's, and a constant $I_{\max}$ requires the JJ's to be very short so that I_c has a negligible field dependence. We could not use the symbol I_c here, since ''critical current'' will be referred to only for the critical state of the entire array. Also, we make normalization of $I_{\max}$, H, and H_{ij} consistently to one flux quantum per void area. Note that there is a relation, $2\pi i_{\max} = \beta$, between $i_{\max}$ and β, which was used in some other works such as Ref. 18.

[13] D.-X. Chen and A. Hernando, Phys. Rev. B **49**, 465 (1994).

[14] D.-X. Chen, A. Sanchez, and A. Hernando, Phys. Rev. B **50**, 10 342 (1994).

[15] C. P. Bean, Phys. Rev. Lett. **8**, 250 (1962).

[16] J. M. Greene, J. Math. Phys. **20**, 1183 (1979).

[17] S. N. Dorogovtsev and A. N. Samukhin, Europhys. Lett. **25**, 693 (1994).

[18] F. Parodi and R. Vaccarone, Physica C **173**, 56 (1991).

[19] D.-X. Chen, A. Sanchez, and A. Hernando, Physica C **250**, 107 (1995).

[20] D.-X. Chen, A. Sanchez, and A. Hernando, Physica C **244**, 123 (1995).